An In-Depth Analysis of Power-System-in-Inductor (PSI²) Technology for Power Module Packaging

Andrew Yurek, Wenbo Liu, Yan-Fei Liu, *Fellow*, *IEEE*
Department of Electrical and Computer Engineering
Queen's University, Kingston, Canada
13aty@queensu.ca, liu.wenbo@queensu.ca, yanfei.liu@queensu.ca

Abstract— This paper provides a thorough analysis of the power-system-in-inductor (PSI²) packaging for power modules through FEA simulation and experimentation of electrical and thermal performance. To sufficiently analyze the PSI² packaging, all tests conducted compare performance of PSI² to conventional plastic epoxy packaging using identical buck power modules. PSI² uses magnetic material as both the power module packaging and magnetic inductor core to increase inductor winding size and thermal conductivity of the package. In experimental testing the PSI² package achieves 2.82% greater efficiency, 0.48W less loss, 23.9°C lower top temperature, and 3.5°C lower bottom temperature at full load compared to the plastic package. Constant loss experimentation reveals approximately one third of the surface temperature difference is the result of the PSI² improved thermal conductivity at full load.

Keywords— *PSI²; power system; power module; thermal; low loss; FEA simulation*

I. INTRODUCTION

In electronic devices today, point of load (POL) DC-DC power conversion is handled by buck converters. One struggle with point of load converters is the ability to transfer heat away from the junctions in small packages. Higher switching frequencies are required to keep the size of the inductors and capacitors small to reduce the overall package size. This results in greater switching losses and requires research towards modelling and reducing thermal dissipation [1] [2] [3] [4]. Significant research has focused on developing different methods of transferring and reducing heat from integrated point of load converters [5] [6] [7] [8] [9] [10] [11] [12] [13]. Low-temperature cofire ceramic (LTCC) is used to integrate power supplies and inductors at high power [7] [8] [9] [13]. At very low power, the inductor has been integrated into the substrate of the PCB to achieve integrated power delivery [10]. Recently, research has focused on developing an integrated power module called power-system-in-inductor (PSI²) [6] [11] [12]. This system integrates passive components into the cavity of the inductor core, reducing volume and increasing thermal conductivity.

Thermal energy is generated in POL converters through DC and AC losses of the main components. DC losses consist of conduction losses of the IC, power MOSFETs, inductor, and filter capacitors. AC losses consist of hard-switching losses of the MOSFET's and the AC winding and core losses of the inductor. The loss must be reduced to minimize module size,

lower component cost, and decrease the required thermal dissipation. The remaining heat generated by the loss must be dissipated through the POL package to avoid thermal throttling and improve the lifespan of the device.

The PSI² package is designed to address the loss and thermal challenges faced by POL converters. The PSI² package accomplishes these objectives by replacing the traditional plastic packaging with the magnetic inductor core. This design allows for the size of both the winding and core of the inductor to increase, thereby decreasing winding and core losses. In addition, the magnetic core offers much greater thermal conductivity compared to plastic, thereby improving thermal dissipation. The PSI² package achieves these results while maintaining package volume. The objective of this paper is to determine the extent of these benefits using buck power modules with PSI² or plastic package. The PCBs, components, and testing environment are identical for both power modules to isolate all external influences during testing. Various simulation and experimentation are conducted to further verify the exact benefit of PSI² over traditional plastic package.

This paper is organized into the following three sections: Section II describes the package design and the module fabrication, Section III presents the simulated thermal results using FEA analysis, Section IV presents the thermal and electrical experimental results, and Section IV concludes the findings of this paper.

II. DESIGN AND FABRICATION OF THE POWER MODULES

This section will introduce the design and fabrication of the power modules for both packaging types. The typical packaging of power modules involves fixed components soldered to a PCB with plastic epoxy encapsulation. The plastic acts as both a heatsink and a protective casing for the module. Fig. 1 (a) shows the plastic module with the plastic covering removed for visibility. The new PSI² packaging method uses the same structure as the plastic package except the epoxy is replaced with the magnetic inductor core. The PSI² package encapsulates the power module using the core of the inductor. Components are contained in the cavity of the core opposite the inductor windings. Fig. 1 (b) shows the PSI² module with the inductor core removed for visibility. The IC embedded in the cavity is thermally connected to the magnetic core using thermal paste with the same conductivity as the plastic package.

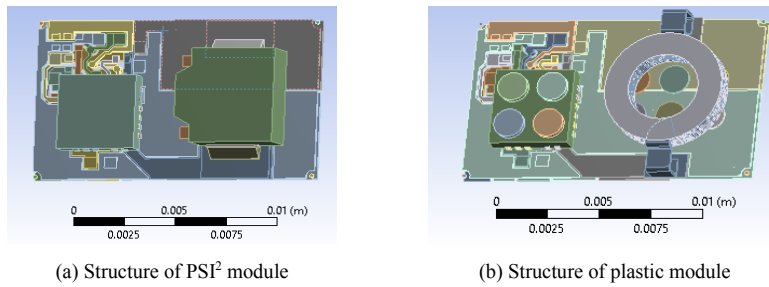(a) Structure of PSI² module   (b) Structure of plastic module

Fig. 1. PCB structure of power modules with cases removed

The topology of the power modules are buck converters with constant on-time and variable frequency. The testing parameters are listed in Table 1. These power modules consist of an IC with two switching MOSFET's, an inductor, and passive components for filtering and control. The fixed inductor is selected based on the dimensions of the PSI². Both packages are designed with the same size restrictions to ensure fair results. The selected PSI² package has an overall LWH of 15x9x3mm. The fixed inductor for the plastic package must be less than 2mm tall to allow for the epoxy coating to cover the entire package. For inductor selection, the minimum current rating is 8.6A and minimum current saturation rating is 9.5A. This allows the inductor to operate unsaturated within the full load condition (8A). The inductance is selected to be 1uH. The PSI² package inductor was designed for these specifications, therefore the fixed inductor in the plastic package must also meet the same physical and electrical requirements to allow for fair comparison. A commercial 1uH, 8.6A, 17.2 mOhm fixed inductor is selected for the plastic package to meet these criteria.

Table 1: Device specifications for the tested POL converters.

Topology	Input (V)	Output (V)	Full Load (A)	$T_{ambient}$ (°C)
Buck Converter	6, 12, 24	1, 1.5	8	22

The PCB's are manufactured before being populated with components. The plastic package has larger inductor footprints on the top side to accommodate the fixed inductor. Thermal vias are dispersed throughout the power planes to transfer heat to the bottom side of the board. For the PSI² package, the inductor is soldered on last to encapsulate the components. Fig. 2 (a) shows the fabricated PCBs of both power modules. These PCBs are made identical, except for the inductor, to provide the most accurate and fair testing results. Fig. 2 (b) shows the populated plastic power module without the plastic cover. The PSI² package is not shown as the inductor cover inhibits visibility.
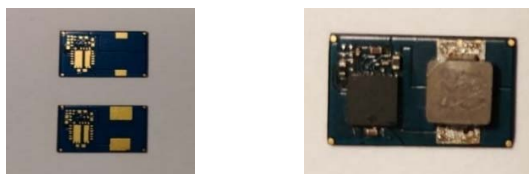
(a) PSI² (top) and Plastic (bottom)   (b) Plastic, populated

Fig. 2. Fabricated power modules for PSI² and plastic packages.

The PSI² module and plastic pack are soldered onto the identical testing boards. The testing board provides a heatsink for the modules and allows for the mounting of larger passive components such as large capacitors and lower tolerance resistors. Finally, epoxy is poured onto the plastic package using a small plastic mold to encapsulate the module.

III.   FEA THERMAL SIMULATION

In this section, the two prototype modules are modelled and simulated in Ansys FEA thermal simulation. To simulate both power modules in FEA analysis, the loss of converter must be known. For the buck power modules, the major contributors to loss are the core loss, winding loss, and loss in the IC. To calculate core loss, ANSYS Maxwell simulation was used. The inductance, turns, area of core, and the waveform of the winding current are required to simulate the core loss. Using ANSYS Maxwell electromagnetic simulation, the waveform of the B field and core loss of the inductor can be obtained. Since the inductance, turns, and area of core are known parameters of the selected inductors, the remaining variable to define is the winding current. To define the winding current, the inductor voltage waveform is derived and applied to the winding input terminals. Since the winding current is a function of applied winding voltage, the winding current can be simulated using the winding voltage waveform. For a buck converter, the inductor voltage is equal to $V_{in}-V_{out}$ during ON time, and $-V_{out}$ during OFF time. The input and output voltage values are known for all operating conditions. To calculate the core loss character, Pv, the simulation uses the Steinmetz equation with coefficients supplied by the user. The Steinmetz coefficients were estimated based on core material. The final core loss for the given inductor volume is calculated using equation (1).

$$P_{core} = P_v A L_e \qquad (1)$$

Therefore, the core loss was successfully calculated for 1V and 1.5V output voltage condition using electromagnetic simulation.

Winding loss is the second key loss contributor that must be calculated. Winding loss is calculated using equation (2).

$$P_{winding} = I_{out}^2 R_{winding} \qquad (2)$$

The output current is a known, with full load current equal to 8A. The winding resistance is defined in the datasheets of both converters as the DCR. For PSI², the DCR is rated as 12mΩ. For

the fixed inductor, the DCR is rated as 17mΩ. The resistance of the winding is affected by DC and AC influences, in this case skin effect and temperature. Therefore, the DCR is tested for both packages' inductors around the switching frequency of the converter. The real DRC is measured at 15mΩ and 21mΩ for the PSI² and fixed inductor, respectively. The resistance change due to temperature is estimated based on datasheet waveforms and simulation results and is selected at a 1.5 factor for both inductors. Therefore, the winding loss is accurately estimated for different load conditions.

The final key loss contributor is due to the power modules' IC. The key contributor to thermal generation in the IC is the integrated switching MOSFETs. MOSFET loss consists of switching and conduction loss. Since the power modules operate with hard switching, switching loss is dominant and dependent on operating frequency. The same IC and load current are used in both converters, therefore differences in IC loss should only depend on the frequency dependent switching loss. The loss of IC was estimated as the remaining amount of total loss after accounting for core and winding loss.
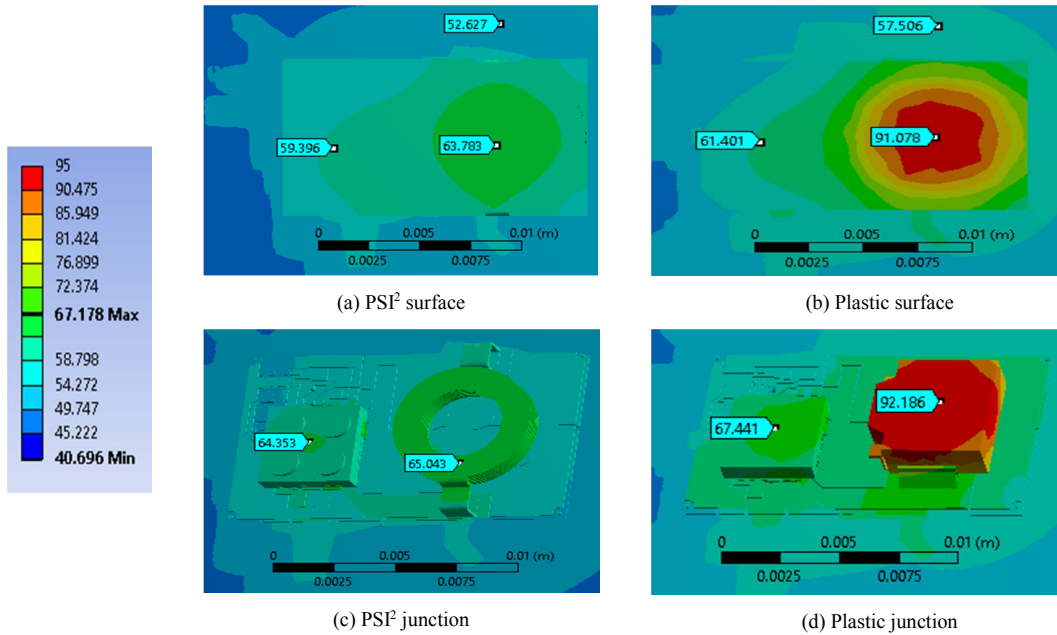

(a) PSI² surface   (b) Plastic surface

(c) PSI² junction   (d) Plastic junction

Fig. 3. Thermal simulation results of surface and junction temperatures at 1V, 8A output.

(a) PSI² surface   (b) Plastic surface
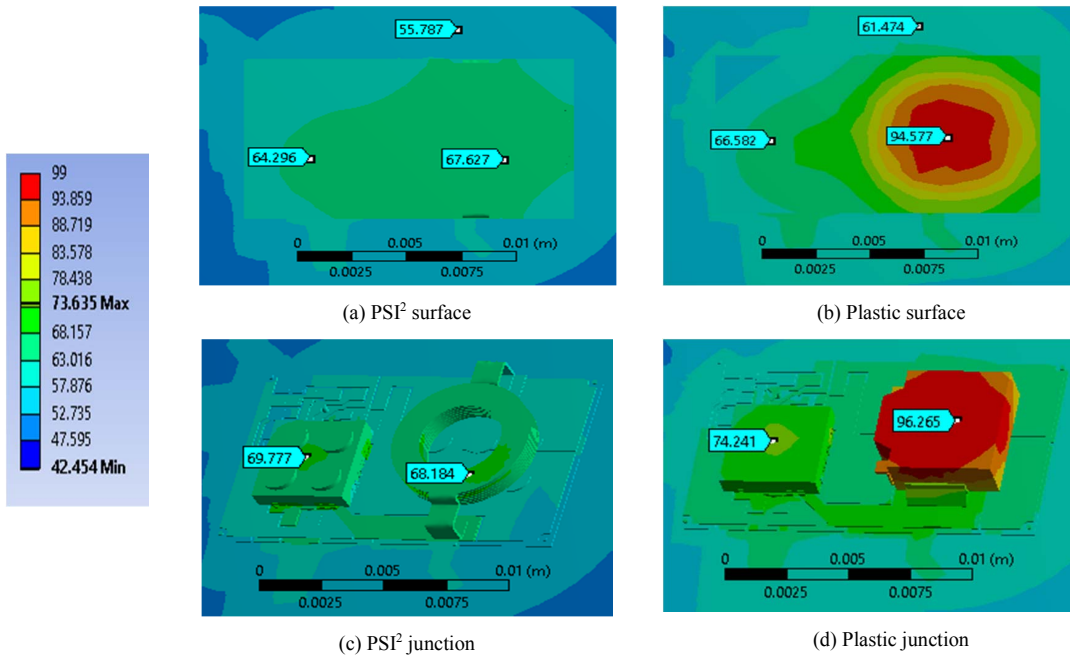
(c) PSI² junction   (d) Plastic junction

Fig. 4. Thermal simulation results of surface and junction temperatures at 1.5V, 8A output.

Thermal performance of both converters is simulated using FEA in ANSYS based on the losses calculated for each package. The materials used, and corresponding thermal conductivities are listed in Table 2. The PSI^2 package offers a 10-fold increase in thermal conductivity compared to plastic. Fig. 3 (a) and (b) show results for 1V output. The peak surface temperature of the plastic package is 27.4°C greater than the PSI^2 package. The temperature variation across the package surface is 4.4°C for PSI^2 compared to 29.7°C for plastic. The surface temperature of the PSI^2 package is more uniform than the plastic package due to the improved thermal conductivity of the PSI^2 package. Fig. 3 (c) and (d) show the junction temperatures of the power modules. The temperature of the plastic package IC is about 3°C greater than PSI^2, while the inductor is 27.2°C. As expected, the major source of loss is due to winding loss in the inductor. The temperature difference of the IC is small due to identical IC's and similar switching frequency. Fig. 4 shows similar results at 1.5V output compared to 1V because only IC and core loss change in this case, and both converters have the same IC and similar core loss.

Table 2. Material thermal conductivity.

Material	Thermal Conductivity
PSI^2 Package (MP55 core)	3 W/(m·k)
Plastic Package	0.3 W/(m·k)
Copper	400 W/(m·k)
FR-4 Epoxy	0.3 W/(m·k)
Ferrite	4 W/(m·k)
Silicon	148 W/(m·k)
Solder	48 W/(m·k)

## IV.   EXPERIMENTAL RESULTS

In this section, the two prototype modules are experimentally tested to measure the performance of the module in terms of efficiency, loss, and thermal performance. The modules are tested using the fabricated module boards mounted to the testing boards described in Section II. Programmable DC power supplies and DC loads are used to vary the input voltage and load current of the power modules autonomously. For each of the 3 input voltage cases, 6.5V, 12V and 24V, the results are averaged to evaluate the performance of each module across the range of operating input voltages. The PSI^2 module mounted to the testing board is shown in Fig. 5.


Fig. 5. PSI^2 module mounted to testing board.

Fig. 6 below show the efficiency curves for the 12V nominal input case at 1V and 1.5V output respectively. The PSI^2 benefits from the magnetic package by allowing for a larger inductor, and lower DCR in the windings. The result is that the PSI^2 package is more efficient and has lower loss. Across all input and output voltage cases, the PSI^2 package has a greater efficiency of 1.82% overall, and 2.82% at full load compared to the plastic package.
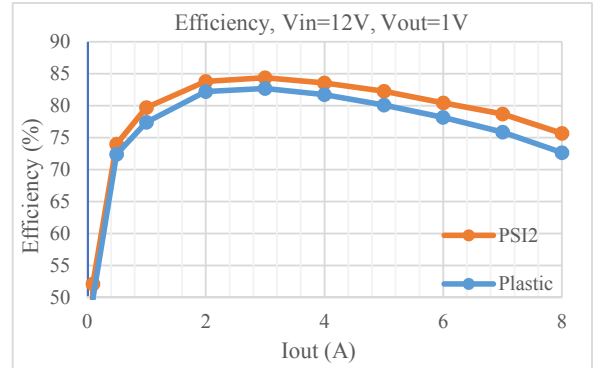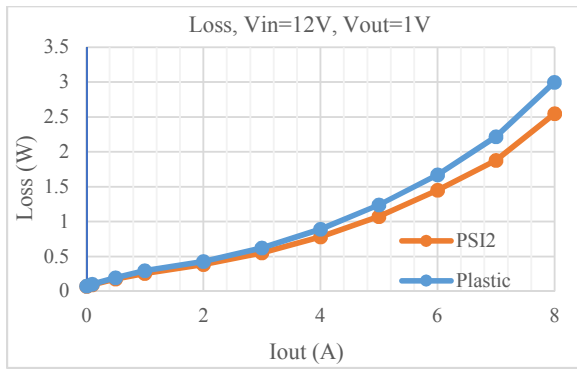

(a) Efficiency vs. load current, 1V output.
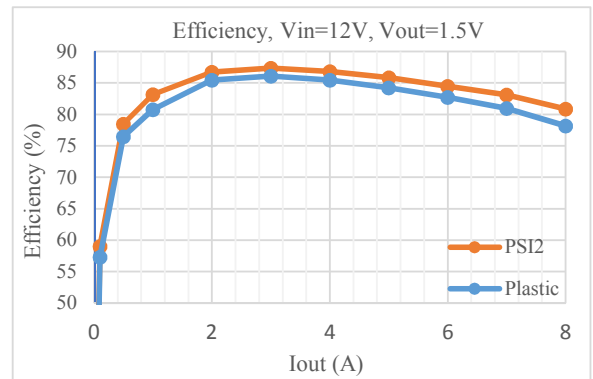
(b) Efficiency vs. load current, 1.5V output.

Fig. 6. Comparing efficiency at different load currents.

The loss of the power module is also calculated while measuring the efficiency. Fig. 7 below shows the loss curves for the 12V nominal input case at 1V and 1.5V output respectively. Overall, the PSI^2 package has 0.14W less loss than the plastic package across all input and output voltage cases. At full load, the PSI^2 module has 0.48W less loss than plastic module A summary of these results is shown in Table 4. These averages are aggregated for the three input voltage cases. These results show that the PSI^2 package offers better electrical performance compared to the traditional plastic packaging. The PSI^2 package has the advantage of using package volume more efficiently to allow for larger inductor coil windings and consequently lower DCR. The PSI^2 package therefore achieves less loss and greater efficiency compared to the plastic package.
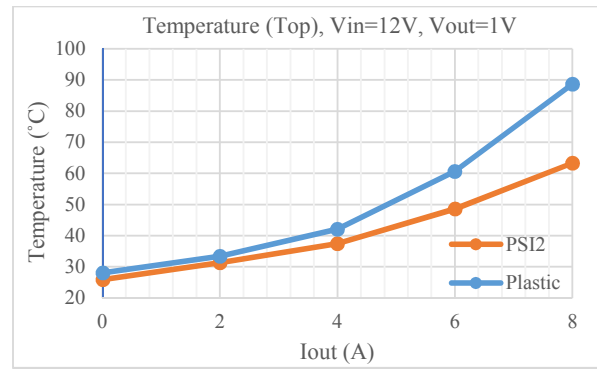
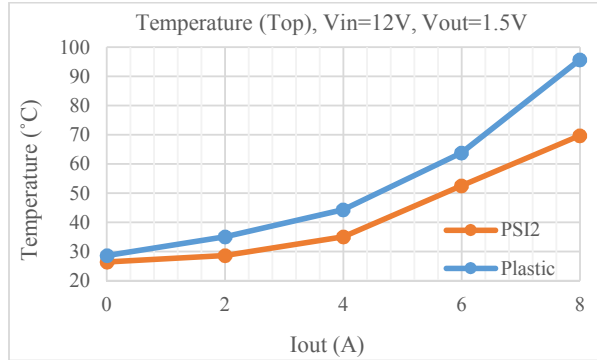(a) Loss vs. load current, 1V output.
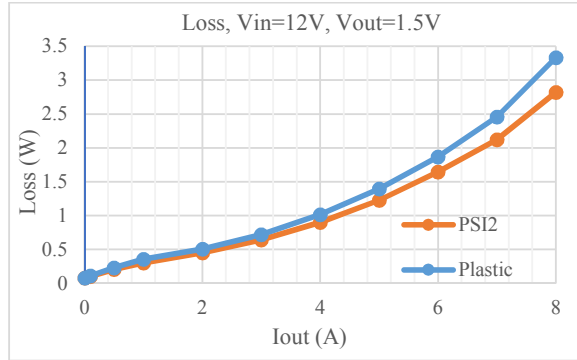
(b) Loss vs. load current, 1.5V output.

Fig. 7. Comparing loss at different load conditions.
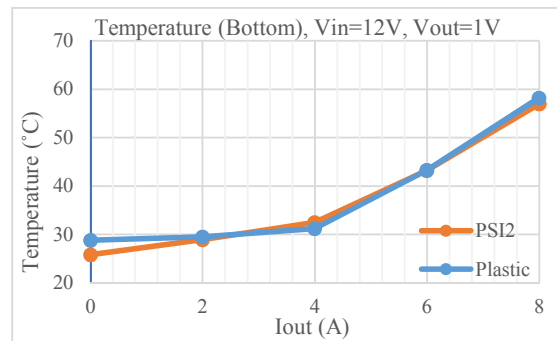

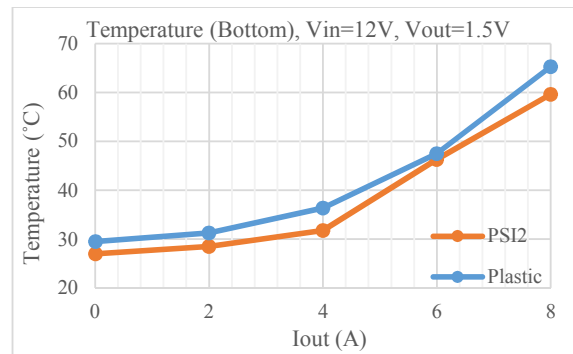(a) Top temperature vs. load current, 1V output.

(b) Top temperature vs. load current, 1.5V output.

Fig. 8. Comparing top temperatures at different load conditions.

(a) Bottom temperature vs. load current, 1V output.

(b) Bottom temperature vs. load current, 1.5V output.

Fig. 9. Comparing bottom temperatures at different load conditions.

The top and bottom temperature of the PSI^2 and plastic power modules are measured using thermal cameras under different operating conditions. Temperature data is collected from the top of the module and the bottom of the testing board. A small coating of epoxy is put on the top of the PSI^2 package to guarantee the same emissivity is observed by the thermal camera for both modules. The first test involves measuring the temperature of the modules under the same load current conditions. The output current is set between 0 and 8A in steps of 2A. Overall, the PSI^2 package is on average 8.42°C cooler than the plastic on top and 0.8°C cooler on the bottom for both output voltages. At full load, the PSI^2 package is 23.9°C cooler than the plastic on top, and 3.5°C cooler on the bottom for both input voltages. A full summary of the results can be seen in Table 3 below. Fig. 8 shows the PSI^2 and plastic modules top temperatures versus load current. The top temperature disparity can be attributed to poor thermal conductivity of the epoxy and higher DCR in the fixed inductor than the PSI^2. Fig. 9 shows the bottom temperatures of the test board for both modules versus load current. The bottom temperatures of both packages are similar due to the almost identical PCB layouts. Most of the heat being transferred to the bottom of the board is through the footprints of the components of the PCB. The IC is the component with the largest footprint and will therefore transfer the most heat to the bottom of the board. Since both modules use the same IC and operate at a similar switching frequency, it is expected that the bottom temperatures will be similar.

Thermal images are captured to show the thermal performance of both packages. The top sides of both packages are coated with epoxy to ensure the same emissivity is observed by the thermal camera. Thermocouple measurements are used to validate the thermal camera results. Fig. 10 shows that the plastic module is the hottest with 25.4°C higher temperature compared to the PSI^2 module at 1V output, 8A load. The lower DCR of the PSI^2 inductance and larger thermal conductivity of the PSI^2

package contribute to these results. The same result can be seen in Fig. 11, where the PSI^2 is 26°C cooler than the plastic package at 1.5V output, 8A load. The temperature difference from 1V to 1.5V is almost identical due to most additional loss being primarily generated in the IC due to increased switching loss. This result agrees with the simulated results generated in Section III.
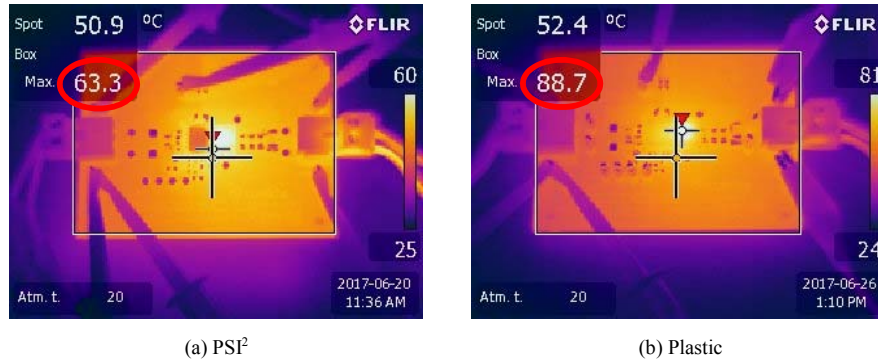

(a) PSI^2 (b) Plastic

Fig. 10. Thermal images of the PSI^2 and plastic packages at 1V, 8A output.
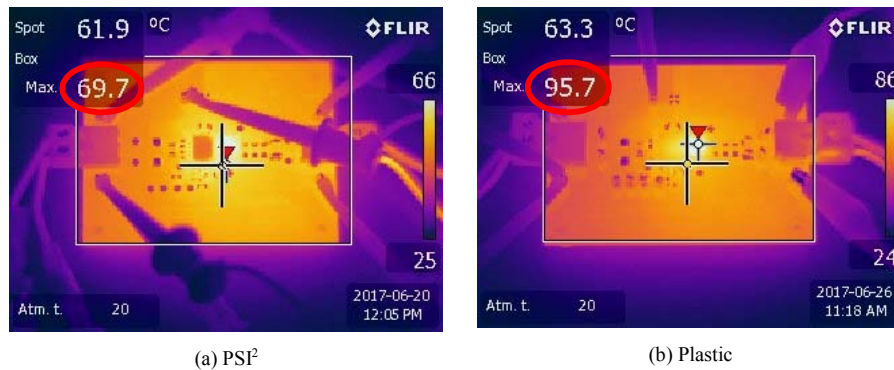

(a) PSI^2 (b) Plastic

Fig. 11. Thermal images of the PSI^2 and plastic packages at 1.5V, 8A output

Comparing the simulation results from Section III, the experimental results are similar. At 1V output, the simulated temperature for the PSI^2 module is about 0.5°C hotter than the experimental result. For plastic, the simulated temperature is about 2.3°C hotter than the experimental result. At 1.5V output, the PSI^2 simulation is 2°C cooler, while plastic simulation is 1°C cooler. The simulation verifies the experimental results within a margin of error. Error is introduced from estimations in loss calculations and incalculable losses in experimental testing. A summary of the results is shown in Table 3.

Table 3: Simulated versus experimental thermal results.

Package	V_{out}=1V, I_{out}=8A	V_{out}=1.5V, I_{out}=8A
PSI^2 (simulated)	63.8°C	67.6°C
PSI^2 (experimental)	63.3°C	69.7°C
Plastic (simulated)	91.1°C	94.6°C
Plastic (experimental)	88.7°C	95.7°C

The final test involves operating both modules with constant loss. The objective of this test is to isolate the heatsinking qualities of both packages from the electrical qualities of the respective package inductors. For this test, the loss of the modules is fixed at one, two and three watts. In this way, both modules will be generating the same quantity of heat; therefore, the surface temperature difference will be the result of the thermal conductivity of the package. The input and output voltages are the same for both modules. The input voltage is set to 24V to allow both modules to produce three watts of loss. The test procedure otherwise remains the same, except loss is varied instead of load current. The top temperatures are shown in Fig. 12. Across both 1V and 1.5V input voltages, the PSI^2 package is on average 8.68°C cooler than the plastic package on top. The bottom temperatures are shown in Fig. 13. The PSI^2 package is on average 1.4°C cooler on the bottom of the testing board. In the temperature versus load current test, the average top temperature difference at full load was 23.9°C compared to 8.68°C at constant loss conditions. Therefore, the temperature

difference between the PSI^2 and plastic package is predominately due to less winding loss. However, the constant loss tests show that the thermal conductivity of the package accounts for approximately one third of the average temperature difference across the range of output voltage and power conditions. Thus, both the lower loss components and improved thermal conductivity of that the PSI^2 package contribute significantly to the overall improved performance compared to a plastic package. On the bottom side, the average temperature difference is very small. This is expected considering most heat transfers to the bottom of the board through the identical layouts and footprints of both boards. Additionally, the core and IC loss is very similar for both packages which are the chief contributors to bottom side heat.
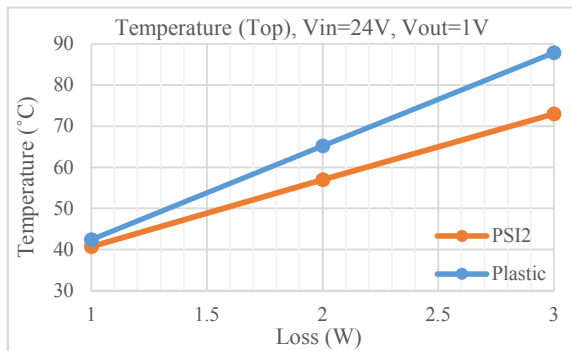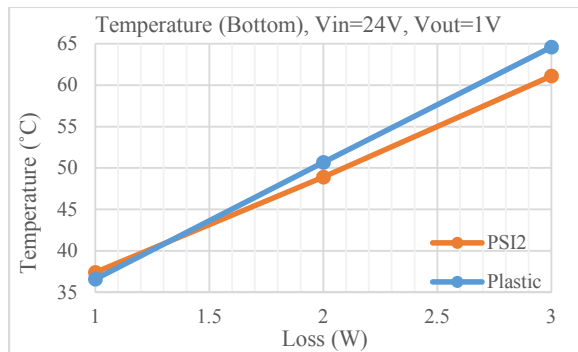
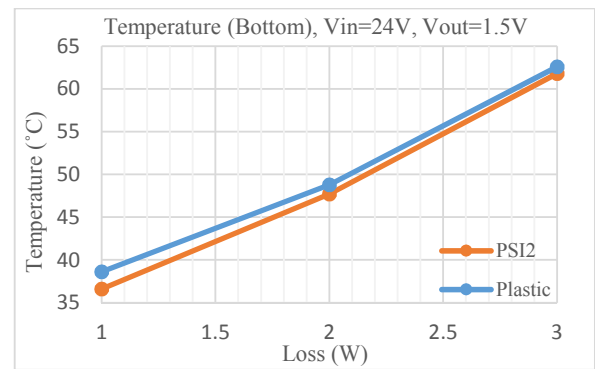

(a) Top temperature vs. loss, 1V output.
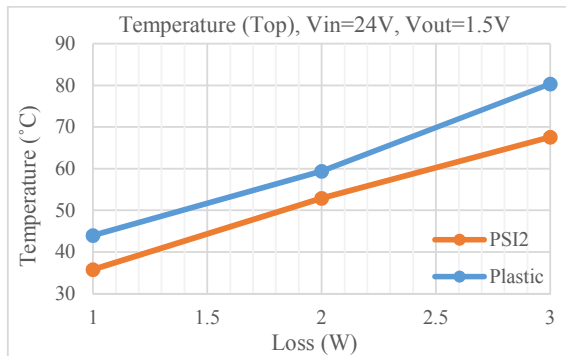
(b) Top temperature vs. loss, 1.5V output.

Fig. 12. Top temperatures at different loss conditions.

(a) Bottom temperature vs. loss, 1V output.

(b) Bottom temperature vs. loss, 1.5V output.

Fig. 13. Bottom temperatures at different loss conditions.

A summary of the results is shown in Table 4 below. For all tests, the values for the plastic package are subtracted from the PSI^2 package (PSI^2-Plastic).

Table 4: Experimental results of PSI^2 versus plastic power modules.

Test	Difference (PSI^2-Plastic)
Efficiency	1.82 %
Full Load Efficiency	2.82 %
Loss	-0.14 W
Full Load Loss	-0.48 W
T_{Top}	-8.42 °C
T_{Bottom}	-0.8 °C
Full Load T_{Top}	-23.9 °C
Full Load T_{Bottom}	-3.5 °C
Constant Loss T_{Top}	-8.68 °C
Constant Loss T_{Bottom}	-1.4 °C

V. CONCLUSIONS

This paper evaluates the thermal and electrical performance of the PSI^2 package by comparing against the traditional plastic package through a new accurate experimentation with identical buck power modules. The PSI^2 package replaces the plastic cover and inductor of the traditional power module with a magnetic package that acts as the inductor core and package cover. FEA thermal simulations are conducted on the identical power modules to estimate the thermal performance of both packages and validate the experimental results. Experimental testing is conducted with identical power modules to more accurately validate the improved electrical and thermal performance offered by the PSI^2 package through constant load and constant loss tests. Overall, the PSI^2 package achieves greater efficiency, less loss, lower top temperature, and lower bottom temperature compared to the plastic package. The experimentation proves that these results are the product of both the improved electrical and thermal performance offered by the PSI^2 package.

References

[1] T. Girasek, A. Pietrikova, T. Welker and J. Muller, "Improving thermal resistance of multilayer LTCC module with cooling channels and thermal vias," in *Electronics Technology (ISSE), 2017 40th International Spring Seminar on*, Sofia, Bulgaria, 2017.

[2] M. Orabi and A. Shawky, "Proposed Switching Losses Model for Integrated Point-of-Load Synchronous Buck Converters," *IEEE Transactions on Power Electronics,* vol. 30, no. 9, pp. 5136-5150, 2014.

[3] Y.-F. Liu, W. Eberle, Z. Zhang and P. C. Sen, "A simple analytical switching loss model for buck voltage regulators," in *Applied Power Electronics Conference and Exposition*, Austin, TX, 2008.

[4] K. Ma, A. S. Bahman, S. M. Beczkowski and F. Blaabjerg, "Loss and thermal model for power semiconductors including device rating information," in *2014 International Power Electronics Conference*, Hiroshima, Japan, 2014.

[5] P. Artillan, M. Brunet, D. Bourrier, J.-P. Laur, N. Mauran, L. Bary, M. Dilhan, C. Alonso and J.-L. Sanchez, "Integrated LC Filter on Silicon for DC–DC Converter Applications," *IEEE Transactions on Power Electronics,* vol. 26, no. 8, pp. 2319-2325, 2011.

[6] J. A. Herbsommer, J. Noquil, O. Lopez and J. Sherman, "Integration of power semiconductors devices: Synchronous buck converters in a package," in *Applied Power Electronics Conference and Exposition (APEC)*, Orlando, FL, 2012.

[7] F. C. Lee, D. Reusch and S. Ji, "High-Frequency High Power Density 3-D Integrated Gallium-Nitride-Based Point of Load Module Design," *IEEE Transactions on Power Electronics,* vol. 28, no. 9, pp. 4216-4226, 2013.

[8] Q. Li and F. C. Lee, "High Inductance Density Low-Profile Inductor Structure for Integrated Point-of-Load Converter," in *IEEE Applied Power Electronics Conference and Exposition*, Washington, DC, 2009.

[9] Q. Li, Y. Dong, F. C. Lee and D. J. Gilham, "High-Density Low-Profile Coupled Inductor Design for Integrated Point-of-Load Converters," *IEEE Transactions on Power Electronics,* vol. 28, no. 1, pp. 547-554, 2013.

[10] J. Sun, D. Giuliano, S. Devarajan, J.-Q. Lu, T. P. Chow and R. J. Gutmann, "Fully Monolithic Cellular Buck Converter Design for 3-D power Delivery," *IEEE Transactions On Very Large Scale Integration (VLSI) Systems,* vol. 17, no. 3, pp. 447-451, 2009.

[11] L. Wang, D. Malcolm and Y.-F. Liu, "An innovative power module with power-system-in-inductor structure," in *Applied Power Electronics Conference and Exposition*, Long Beach, CA, 2016.

[12] L. Wang, D. Malcolm, Y.-F. Liu and W. Liu, "Thermal Analysis of a Magnetic Packaged Power Module," *Applied Power Electronics Conference and Exposition (APEC), 2012 Twenty-Seventh Annual IEEE,* pp. 2095-2101, 2016.

[13] Y. Su, Q. Li and F. C. Lee, "Design and Evaluation of a High-Frequency LTCC Inductor Substrate for a Three-Dimensional Integrated DC/DC Converter," *IEEE Transactions on Power Electronics,* vol. 28, no. 9, pp. 4354-4364, 2012.